

# Characterization the Optical Band Gap of Indium Tin Oxide based on Different Thickness

**Azmira Roziana Lai<sup>1</sup>, Ahmad Hadi Ali<sup>2\*</sup>, Nooriskandar Sani<sup>1</sup>, Muhamad Muizzudin Azali<sup>1</sup>**

<sup>1, 2</sup> LASERG, Photonics Devices and Sensor Research Centre (PDSR),  
Department of Physics and Chemistry,  
Faculty of Applied Sciences and Technology,  
Universiti Tun Hussein Onn Malaysia (Pagoh Campus),  
84600 Pagoh, Muar, Johor, MALAYSIA.

\*Corresponding Author Designation

DOI: <https://doi.org/10.30880/ekst.2023.03.01.019>

Received 15 January 2023; Accepted 11 April 2023; Available online 3 August 2023

**Abstract:** There were various transparent conductive oxide that used in various application. Zinc oxide as one of the transparent conductive oxide has poorer conductivity and transparency lower than indium tin oxide. Indium tin oxide as a semiconductor is a commonly used transparent conductive oxide where it has few unique properties where it has high transparency in the visible range, good electrical conductivity and wide bandgap energy. However, the thickness of the indium tin oxide might result in degradation that might affect optical and electrical characterization. In this study, a different thickness of ITO was deposited onto the Si and glass substrates. The samples were characterized based on the optical, electrical and structural properties. From UV-Vis spectrometer, absorbance graphs showed increasing trends with increasing thickness, while transmittance graphs show opposite trends. From four-point probe, the resistivity was inversely proportional to the increase of thickness. The XRD results show the higher the thickness, the greater the intensity. Finally, the AFM results show an increment of the grain size along with the thickness.

**Keywords:** ITO, UV-Vis Spectrometer, Four Point Probe, XRD, AFM.

## 1. Introduction

A crucial scope defines the optical, electronic, carriage and redox characteristics of a grain is called the band gap where it is among the highest energy levels and lowest unoccupied energy levels, but the gap takes place in a lot of types. For instance, the band gap, HOMO-LUMO gap, fundamental gap, optical gap or transport gap with each of these gaps bringing their meaning. If fail to understand the differentiation between these variety energy gaps, it will lead to wrong understanding in the literature which is indicated by the mostly apply of inappropriate words [1]. The incorporation of rare earth ion

doping could improve photocatalytic activity by increasing photocurrent response and electron-hole pair separation under UV illumination [2].

Since it has been widely used as the transparent current spreading electrode for GaN light-emitting diodes and in liquid-crystal displays, indium tin oxide (ITO) is of interest. ITO can also resist the high processing temperatures that are present in many semiconductor processes. Making a good Ohmic contact while working with novel materials like  $\text{Ga}_2\text{O}_3$  is one of the challenges. ITO may help to resolve that problem. Carey and Oshima have previously demonstrated that the development of an Ohmic contact using ITO is possible and can achieve performance levels comparable to those of Ti/Au without the requirement for substantial surface preparation [3].

Material is sputtered from the target and then deposited on a substrate. The procedure is carried out in a closed receiver that has been pushed down to a base vacuum pressure before the deposition process begins. Typically, argon is fed into the chamber at a pressure between 0.5 Pa and 12 Pa to permit plasma ignition. An operating current is determined by the electrode distance and gas pressure. Positive ions would charge the surface of a non-conducting object after bombarding it, which would then shield the electrical field. Ion current would stop flowing. Therefore, only conducting materials like metals or doped semiconductors may undergo the sputtering [4].

In this study, a different thickness of ITOs were deposited onto the Si and glass substrates. The samples were characterized based on the optical, electrical and structural properties.

## 2. Materials and Methods

In this study, ITO thin films were deposited using DC sputtering system model Q150RS. With different deposition time, the ITOs were sputtered onto Si and glass substrates. The film thickness was measured by using ellipsometer [5]. The film thicknesses are 16.5 nm, 37.8 nm, 54.3 nm, 94.5 nm and 156.1 nm. The sputtering current was set at 80 mA. The Si substrates were cleaned with ultrasonic cleaner in acetone solution, isopropyl, distilled water and  $\text{N}_2$  blow before deposition. The Decon-90 glass cleaner was used to clean the glass samples. Then, in a plasma cleaner, they were exposed to RF waves for 15 minutes.

The characterization of ITO thin film starts with UV Vis-Nir spectrophotometer (UV-3600) SHIMADZU spectrometer [6] to determine the optical properties of Indium tin oxide thin film. The wavelength range used in the characterization were 300-800 nm. The electrical properties of indium tin oxide thin film deposited on Si were analyzed by using four-point probe [7]. The structural properties of indium tin oxide thin film deposited on Si were investigated by using Panalytical X-Ray Diffractometer [8]. Moreover, the surface morphological properties of indium tin oxide thin film were studied by Atomic Force Microscopy (AFM) to determine the grain size [9].

## 3. Results and Discussion

The samples were characterized based on its optical, electrical and structural properties. The samples' optical properties were characterized by UV Vis spectrometer while its electrical properties were characterized by four-point probe, its structural properties were characterized by X-ray diffraction (XRD) and the topological characteristics were characterized by atomic force microscope (AFM). The optical data are presented based on graph of absorbance, transmittance and reflectance. The electrical properties are presented based on resistivity. The structural data are presented based on the crystallinity of the layers.

### 3.1 Thickness of ITO Thin Films

Ellipsometer was used to measure the thickness of ITO thin film deposited on Si and glass substrate. The Si/SiO<sub>2</sub> interface has been extensively studied using ellipsometry. As an example, ellipsometric results have indicated that an intermediate layer exists as SiO<sub>x</sub> between an atomically abrupt Si and SiO<sub>2</sub> interface. However, the influence of this intermediate layer is negligible for modeling of thicker films as compared with a few nanometers thick SiO<sub>x</sub>. The database for a SiO layer is tabulated, and both Si/SiO<sub>2</sub> and Si/SiO/SiO<sub>2</sub> models can be chosen for a best fitting of ellipsometric data [10].

Figure 1 shows the thicknesses of ITO thin films measured for different time sputtered. The first one was 300 s deposited ITO where it shows the fitting offers accurate estimation of film thickness, down to sub-monolayer film thicknesses where it was 16.5 nm for 300 s sputter time of ITO. It followed by 725 s deposited ITO where it shows the fitting offers accurate estimation of film thickness, down to sub-monolayer film thicknesses where it was 37.8 nm for 725 s sputter time of ITO. Then it was 1025 s deposited ITO where it shows the fitting offers accurate estimation of film thickness, down to sub-monolayer film thicknesses where it was 54.3 nm for 1025 s sputter time of ITO. Next was the 1750 s deposited ITO where it shows the fitting offers accurate estimation of film thickness, down to sub-monolayer film thicknesses where it was 94.5 nm for 1750 s sputter time of ITO. The 2475 s deposited ITO where it shows the fitting offers accurate estimation of film thickness, down to sub-monolayer film thicknesses where it was 156.1 nm for 2475 s sputter time of ITO.

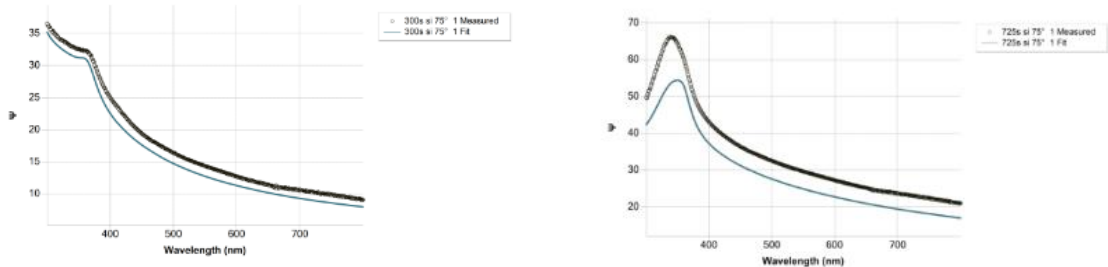
### 3.2 Optical properties of ITO Thin Films

UV-Vis Spectrometry was used to identify the optical properties of ITO thin films. The optical properties are absorbance, transmittance, reflectance and bandgap. The absorbance, transmittance and reflectance of samples were measured in the wavelength range between 300-800 nm. From the optical properties that were measured using UV-Vis spectrometer, the graph of transmittance  $T(\%)$  vs wavelength (nm), the graph of absorbance  $A$  (a.u) vs wavelength (nm) and the graph of reflectance  $R$  (%) vs wavelength (nm) were obtained.

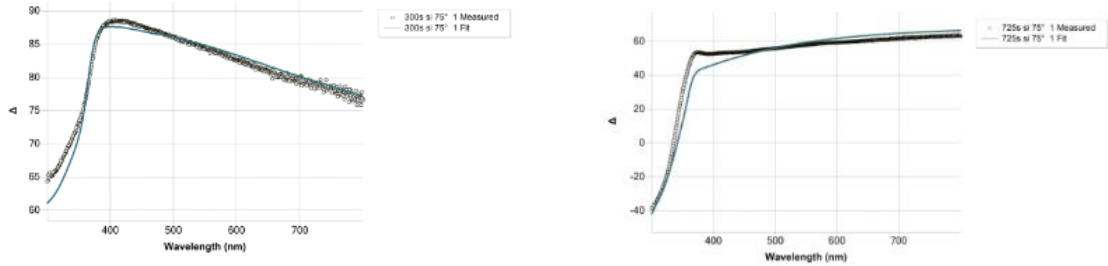
Figure 2 shows the Absorbance  $A$  (a.u) vs Wavelength (nm) graph for different thicknesses of ITO thin film deposited on glass substrate for 16.5 nm, 37.8 nm, 54.3 nm, 94.5 nm and 156.1 nm. From wavelength range of 300-800 nm, the absorbance spectra of ITO thin films show increase trend with the increase of thicknesses. With increasing thickness, free carrier absorption increases carrier concentration in thick film.

Figure 3 shows the  $(h\nu \cdot \alpha)^2$  vs Energy (eV) graph for thickness of 37.8 nm, 54.3 nm and 156.1 nm. Due to the error of measurement while conducting the experiment, the bandgap for thickness of 16.5 nm and 94.5 nm cannot be found using the plotted graph. These observations had been observed by other researchers [11], [12], [13].

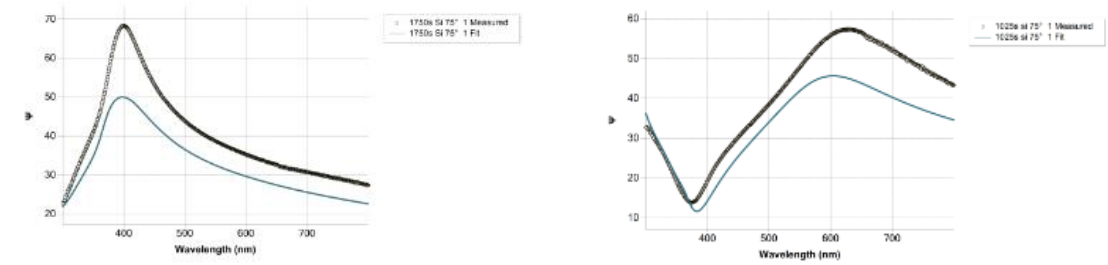
The bandgap values were determine and plotted from the Tauc relation,  $(\alpha h\nu)^2 = h\nu - E_g$  [11]. Additionally, absorbances are related to the bandgap. This is because the tangent of linear part of the plot of  $(\alpha h\nu)^2$  vs  $h\nu$  were used to calculate the values of bandgap for ITO thin films where  $\alpha$  is the absorption coefficient. Table 1 shows the bandgap energy values obtained.



(a)

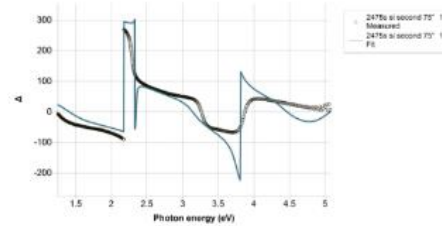
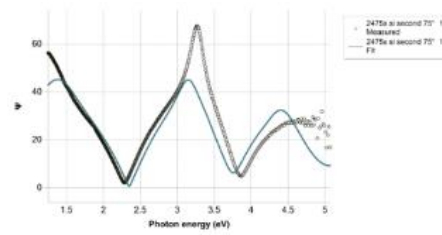


(b)



(c)

(d)



(e)

**Figure 1: Graph of fitting of thicknesses for different sputtering time of ITO**

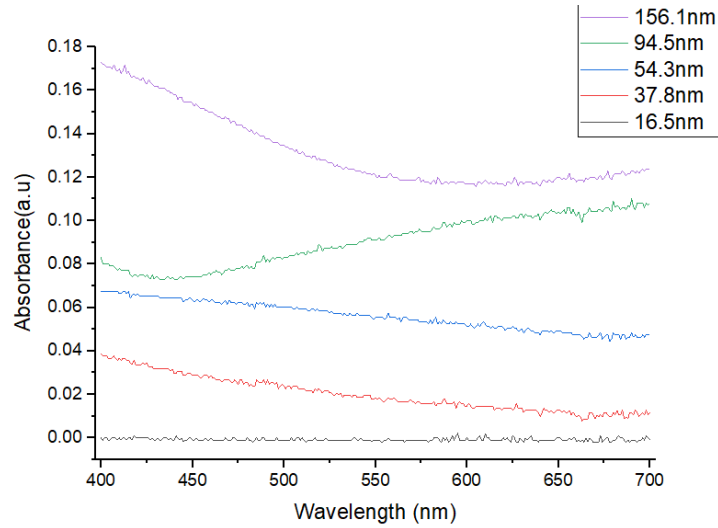


**Figure 2: Graph of absorbance A (a.u) with wavelength (nm) for different thickness of ITO thin films**

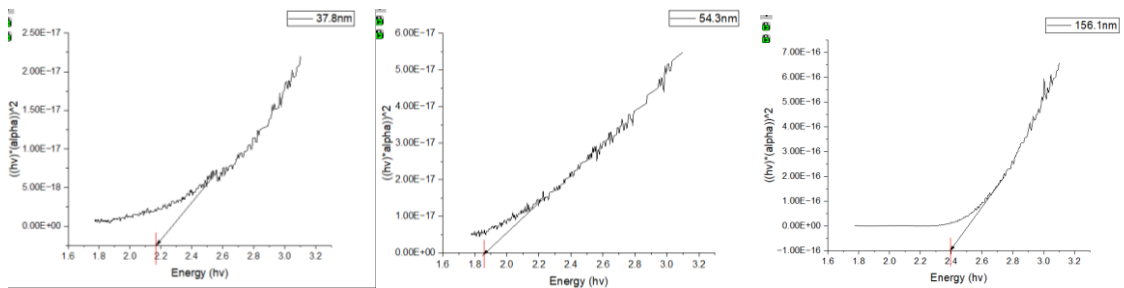
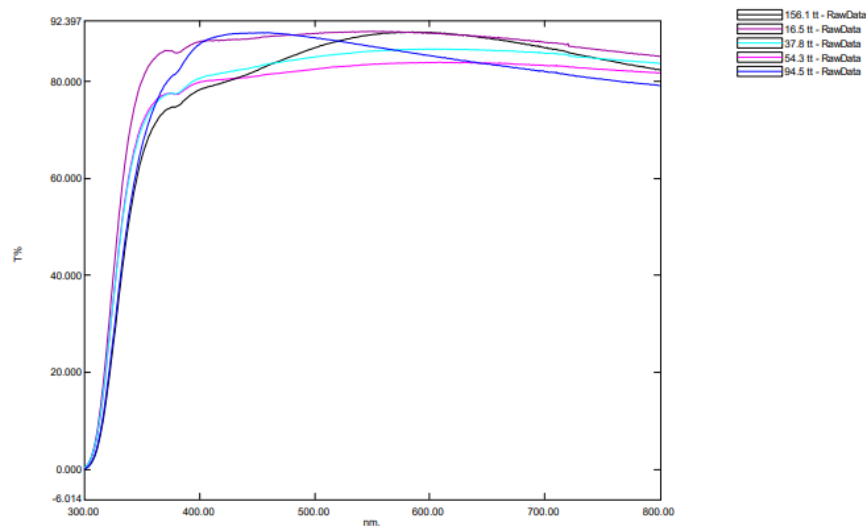


**Figure 3: Graph of  $(h\nu \cdot \alpha)^2$  vs Energy (eV) for various thickness.**

**Table 1: Bandgap values,  $E_g$  of ITO thin films**

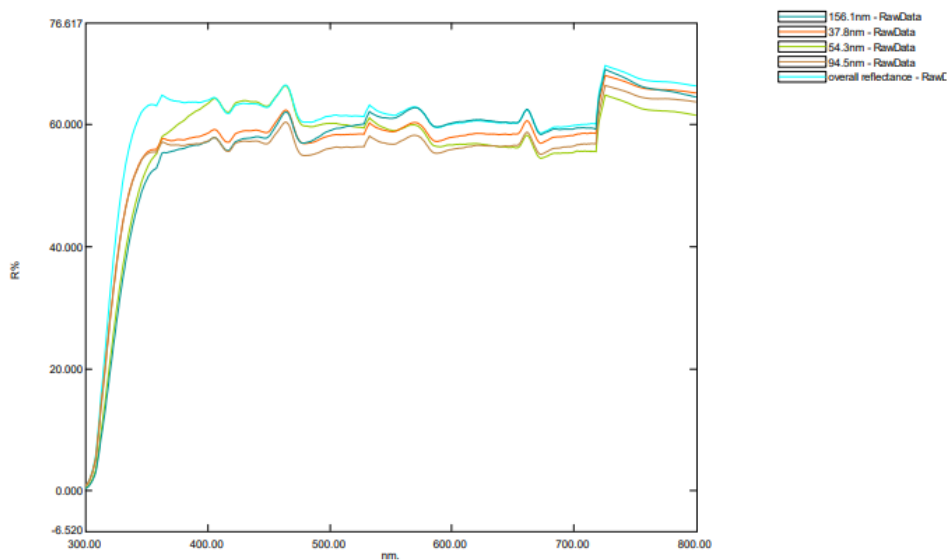
Thickness (nm)	Energy band gap (eV)
37.8	2.18
54.3	1.88
156.1	2.40

Figure 4 shows the transmittance  $t$  (%) vs wavelength (nm) for different thicknesses of ITO for 16.5 nm, 37.8 nm, 54.3 nm, 94.5 nm and 156.1 nm. From wavelength range of 300-800 nm, the transmittance graph seen to be independent with the ITO thicknesses in the visible region. ITO thin films have a properties of high transparency to the visible region. The decrease in thicknesses of ITO thin films with increase of transmittance.



**Figure 4: Graph of transmittance t (%) with wavelength (nm) for various thicknesses of ITO**

Figure 5 shows the graph of reflectance R (%) vs wavelength (nm) for different thicknesses of ITO thin film which were 16.5 nm, 37.8 nm, 54.3 nm, 94.5 nm and 156.1 nm. The reflectance of ITO is proportional to the thickness of ITO thin film so when the thickness is increased from 16.5 nm to 156.1 nm, the reflectance shows a significant growth.



**Figure 5: Graph of reflectance R (%) vs wavelength (nm) for various thickness of ITO**

### 3.3 Electrical Properties of ITO Thin Films

Four-point probe was used to identify the electrical properties of ITO thin films. In this method, the electrical resistivity of thin films of ITO deposited on Si were measured for different thickness. The values of resistivity,  $\rho$  were obtained for this experiment for various thickness of ITO. Figure 6 shows Resistivity ( $\Omega \cdot m$ ) vs thickness of ITO thin film (nm) graph. It is observed that the resistivity decreased

with the increasing of ITO thin film thickness. Hence, it proves that ITO thin film was a good contact material with low resistivity. These observations were also mentioned by [14], [15].

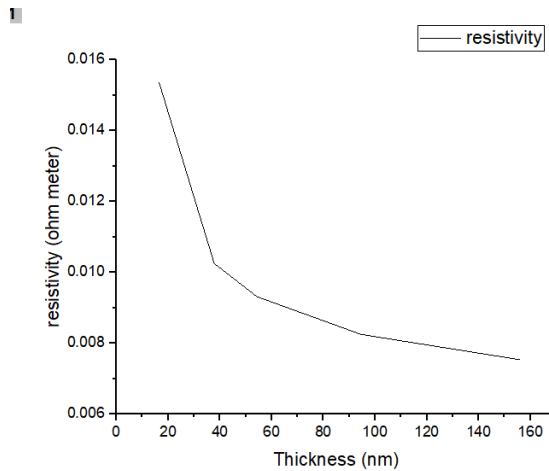


**Figure 6: Resistivity ( $\Omega \cdot m$ ) obtained for various thicknesses of deposited ITO thin film (nm)**

### 3.4 Structural Properties of ITO Thin Films

Figure 7 shows the XRD peaks intensity for various thickness of ITO thin film deposited. In this experiment, by increasing the thicknesses of ITO thin film deposited on Si, the flatness of film was increasing, the electrons of more surface's atoms experience the X-rays. Hence, the intensity of XRD peaks increase when the thickness increase from 16.5 nm to 156.1 nm ascendingly.

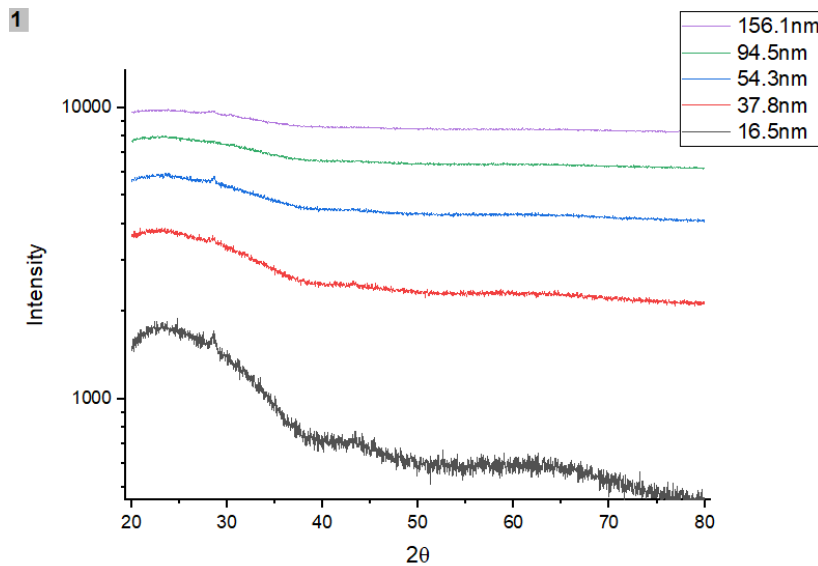


**Figure 7: XRD peak intensity of ITO with various thickness of ITO**

### 3.5 Surface Morphology Properties of ITO Thin Films

For surface morphological properties of ITO thin films, we used Atomic Force Microscopy. We able to determine the material properties from the AFM techniques such as grain size. Figure 8 shows the 2D AFM images of ITO thin films with different thickness. ITO thin films surface show when the

thickness of thin film increase, the film exhibit tiny grain growth by a bit grains. By increasing the thickness of thin films from 16.5nm to 156.1nm, small grains combine then form bigger grains.

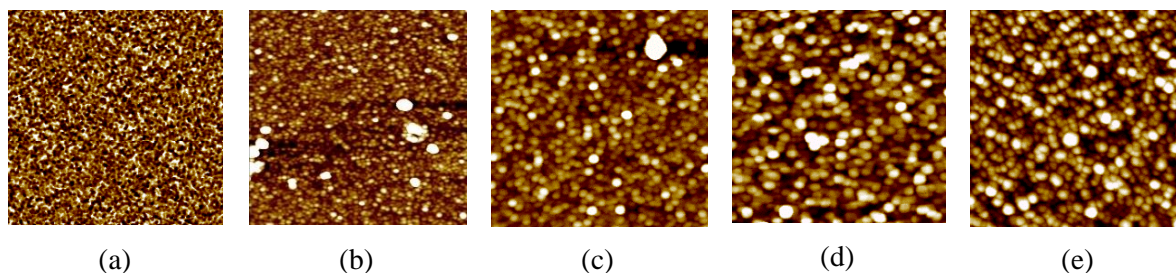


**Figure 8: Surface morphologies of ITO deposited on silicon with various thickness:**  
(a) 16.5 nm, (b) 37.8 nm, (c) 54.3 nm, (d) 94.5 nm, (e) 156.1 nm

#### 4. Conclusion

In this study, the optical, electrical, structural and surface topological properties of ITO thin films were investigated as a function of the film thickness. For 156.1 nm film thickness, the absorbance is 0.053 a.u and the bandgap energy is 2.40 eV. Meanwhile, the resistivity value obtained from four-point probe for 156.1 nm is  $7.53 \times 10^{-3} \Omega \cdot m$ . The peak of XRD is  $28.54^\circ$  for 156.1 nm. Moreover, the surface morphological properties were observed from AFM images. The grain size is the biggest at the highest thickness which is 156.1 nm. Therefore, from this analysis, it is found that the optimum thickness of ITO thin film is 156.1 nm.

#### Acknowledgement

This research was supported by Universiti Tun Hussein Onn Malaysia (UTHM) through TIER 1 Grant Research (Q417) and the Ministry of Higher Education, Malaysia. The authors would also like to thank the Faculty of Applied Sciences and Technology, Universiti Tun Hussein Onn Malaysia for its support.

#### References

- [1] Zanatta A. 2019. Revisiting the optical bandgap of semiconductors and the proposal of a unified methodology to its determination. *Scientifict reports*, 9(1)
- [2] Zhang J, Willis J, Yang Z, Lian X, Chen W, Wang L, Xu X, Lee T, Chen L, Scanlon D, Zhang K, 2022. Deep UV transparent conductive oxide thin films realized through degenerately doped wide-bandgap gallium oxide. *Cell Reports Physical Science*, 100801, 3(3)
- [3] CareyIV P, Pearton S. 2022. Indium-Tin-Oxide Band alignments of dielectrics on (-201)-Ga2O3.
- [4] Liu Z, Liang J, Zhou H et al., 2023. Effect of nitrogen partial pressure on the piezoresistivity of magnetron sputtered ITO thin films at high temperatures. *Applied Surface Science*, 608.
- [5] Goncalves D, Irene D. 2002. Fundamentals and applications of spectroscopic ellipsometry. *Quimica Nova*, 794-800, 25(5).
- [6] UV-Vis-NIR Spectrometer Manufacturer: Shimadzu Model: UV-3600 UV-Vis-NIR Spectrophotometer with Double Beam, Three Detector System Descriptions

- [7] Waremra R, Betaubun P. 2018. Analysis of Electrical Properties Using the four point Probe Method. 73, 13019.
- [8] Bunaciu A, Udriștioiu E and Aboul-Enein H, X-Ray Diffraction: Instrumentation and Applications. 2015. *Critical Reviews in Analytical Chemistry*, 25, 4, 289-299.
- [9] Kyeyune B. 2017. Atomic Force Microscopy. Master Thesis.
- [10] Rasheed M, Barille R. 2017. Optical constants of DC sputtering derived ITO, TiO<sub>2</sub> and TiO<sub>2</sub>:Nb thin films characterized by spectrophotometry and spectroscopic ellipsometry for optoelectronic devices. *Journal of Non-Crystalline Solids*, 1-14, 476.
- [11] Benoy M, Mohammed E, Suresh Babu M, Binu P and Pradeep B. 2009. Thickness dependence of the properties of indium tin oxide (ITO) FILMS prepared by activated reactive evaporation. *Brazilian Journal of Physics*, 629-632, 39(4).
- [12] Khatri R, Vyas S, Patel P, Jani M and Pandya G. 2010. Study of Thickness Dependence Optical Bandgap of InSbBi Thin Films. *International Journal of Physics and Applications*, Vol. 2, No. 3, 95-99.
- [13] Kim Jaeho, Kim Kwangrak and Pakh Heui Jae. 2017. Thickness measurement of a transparent thin film using phase change in white-light phase-shift interferometry. *Current Optics and Photonics*, 505-513, 1(5).
- [14] Li J, Wang Y, Ba D, 2012. Characterization of Semiconductor Surface Conductivity by Using Microscopic Four-Point Probe Technique. *Physics Procedia*, Vol. 32, 347-355.
- [15] Micali M, Cosentino S, Terrasi A. 2021. Structural, optical and electrical characterization of ITO films co-doped with Molybdenum. *Solar Energy Materials and Solar Cells*, 221, 110904.